rocks rich in organic C relative to carbonate weathering over the past ~13 My [31]. Previous interpretations of $^{87}Sr/^{86}Sr$, $^{187}Os/^{186}Os$, and δ^7Li records agree with a change in the nature of weathered material at this time [32].

Many aspects of the biogeochemical Ca^{2+} cycle need to be constrained better by observational and experimental data and paleoceanographic and geologic evidence before a unique interpretation of the causes of the long-term trend and abrupt transitions in $\delta^{44/40}Ca_{seawater}$ is possible. Reconstructions of the global CCD and high-resolution records of seawater Ca^{2+} concentrations (e.g., from fluid inclusions or other proxies) and of the rate of dolomitization and sea-floor generation are all needed.

Our identification of an abrupt middle Miocene change in the $\delta^{44/40}Ca_{seawater}$ record from marine barite attests to the dynamic nature of an element deemed "conservative" in the present ocean and demonstrates that we cannot assume that concentrations of Ca^{2+} in seawater have been stable over the Cenozoic.

References and Notes

1. H. C. Urey, *The Planets, Their Origins and Development* (Yale Univ. Press, New Haven, CT, 1952).
2. A. J. Ridgwell, M. J. Kennedy, K. Caldeira, *Science* **302**, 859 (2003).
3. M. I. Budyko, A. B. Ronov, A. L. Yanshin, *History of the Earth's Atmosphere* (Springer-Verlag, New York, 1987).
4. J. Skulan, D. J. DePaolo, T. L. Owens, *Geochim. Cosmochim. Acta* **61**, 2505 (1997).
5. P. Zhu, J. D. Macdougall, *Geochim. Cosmochim. Acta* **62**, 1691 (1998).
6. T. K. Lowenstein, M. N. Timofeeff, S. T. Brennan, L. A. Hardie, R. V. Demicco, *Science* **294**, 1086 (2001).
7. J. Horita, H. Zimmermann, H. D. Holland, *Geochim. Cosmochim. Acta* **66**, 3733 (2002).
8. J. A. D. Dickson, *Science* **298**, 1222 (2002).
9. P. A. Sandberg, *Nature* **305**, 19 (1983).
10. L. A. Hardie, *Geology* **24**, 279 (1996).
11. H. D. Holland, *Am. J. Sci.* **305**, 220 (2005).
12. C. P. Conrad, C. Lithgow-Bertelloni, *Geology* **35**, 29 (2007).
13. The Ca-isotopic composition of a sample is expressed as the deviation from a standard solution value, using δ-notation in per mil: $\delta^{44/40}Ca = [(^{44}Ca/^{40}Ca_{\text{sample}} - {}^{44}Ca/^{40}Ca_{\text{standard}}) / {}^{44}Ca/^{40}Ca_{\text{standard}}] \times 1000$, where $^{44}Ca/^{40}Ca_{\text{standard}}$ refers to the $^{44}Ca/^{40}Ca$ isotopic ratio of seawater.
14. C. L. De La Rocha, D. J. DePaolo, *Science* **289**, 1176 (2000).
15. A. D. Schmitt, F. Chabaux, P. Stille, *Earth Planet. Sci. Lett.* **213**, 503 (2003).
16. N. G. Sime *et al.*, *Geochim. Cosmochim. Acta* **71**, 3979 (2007).
17. N. Gussone *et al.*, *Geochim. Cosmochim. Acta* **69**, 4485 (2005).
18. M. Amini *et al.*, *Geochim. Cosmochim. Acta* **72**, 4107 (2008).
19. A. Heuser *et al.*, *Paleoceanography* **20**, 10.1029/2004PA001048 (2005).
20. M. S. Fantle, D. J. DePaolo, *Earth Planet. Sci. Lett.* **237**, 102 (2005).
21. J. Farkaš *et al.*, *Geochim. Cosmochim. Acta* **71**, 5117 (2007).
22. A. Paytan, M. Kastner, E. E. Martin, J. D. Macdougall, T. Herbert, *Nature* **366**, 445 (1993).
23. A. Paytan, M. Kastner, D. Campbell, M. H. Thiemens, *Science* **304**, 1663 (2004).
24. A. V. Turchyn, D. P. Schrag, *Science* **303**, 2004 (2004).
25. E. M. Griffith, E. A. Schauble, T. D. Bullen, A. Paytan, *Geochim. Cosmochim. Acta* **72**, 5641 (2008).
26. Range of parameters measured include conditions relevant to the ranges for the measured samples (DSDP-ODP sites): Holocene core-top sample sites include the average annual temperature in the upper 700 m of the water column, where the majority of marine barite is thought to precipitate, 1 to 14°C; the depth of each core-top location, 3175 to 4431 m; water column barite saturation at sea floor, SI = 0.6 to 0.8 and at 700 m, SI = 0.8 to 1.2; average upper (700 m) water column: salinity (34.2 to 34.9), carbonate concentration (86.65 to 139.56 μmol/kg), and dissolved oxygen concentration (1.1 to 6.2 ml/l); bulk sedimentation rate (1.3 to 2.7 cm/thousand years) and barite accumulation rates (0.7 to 23.4 mg m^{-2} year^{-1}).
27. Materials and methods are available as supporting material on *Science* Online.
28. A constant residence time in the model requires that the output flux of Ca^{2+} and the total amount of dissolved Ca^{2+} in the oceans vary together. This is a valid assumption if changes in Ca^{2+} concentration occurred due to changes in the input flux of Ca^{2+} to the ocean that are not accompanied with changes in the C cycle. If a change in Ca^{2+} input flux was associated with and compensated by a change in $CaCO_3$ sedimentation through an increase in alkalinity, no change in Ca^{2+} concentration would result. Increasing or decreasing the residence time by 50% gives similar fluctuations but different magnitudes (peak concentrations range from 180% to 290% of present values) (fig. S5). Modeling the Ca^{2+} system with full carbonate chemistry reveals the sensitivity of the Ca^{2+} cycle to changes in C on long time scales (>10,000 years) [27]. A mechanism for decoupling the two cycles is required in order to result in changes in Ca^{2+} concentration. These might include changes in the rate of dolomitization or the Ca:bicarbonate ratio in the riverine flux due to shifts in the weathering regime.
29. A. Holbourn, W. Kuhnt, M. Schulz, H. Erlenkeuser, *Nature* **438**, 483 (2005).
30. M. Lyle, *Paleoceanography* **18**, 10.1029/2002PA000777 (2003).
31. D. A. Hodell, P. A. Mueller, J. A. McKenzie, G. A. Mead, *Earth Planet. Sci. Lett.* **92**, 165 (1989).
32. E. C. Hathorne, R. H. James, *Earth Planet. Sci. Lett.* **246**, 393 (2006).
33. L. Lourens, F. Hilgen, N. J. Shackleton, J. Laskar, D. Wilson, in *A Geological Time Scale 2004*, F. Gradstein, J. Ogg, A. G. Smith, Eds. (Cambridge Univ. Press, Cambridge, UK, 2004), pp. 409–440.
34. Generated using a smoothing parameter ($P = 0.80$) and data weighted by its precision in the MATLAB 7.6.0.324 (R2008a) cubic smoothing spline function csaps.
35. J. Zachos, M. Pagani, L. Sloan, E. Thomas, K. Billups, *Science* **292**, 686 (2001).
36. Samples provided by the Integrated Ocean Drilling Program. We thank A. Eisenhauer, J. Fitzpatrick, W. A. Griffith, R. Jones, and G. Li for analytical assistance. Supported by NSF CAREER Grant OCE-0449732 (A.P.) and by a National Defense Science and Engineering Graduate Fellowship and an NSF Graduate Research Fellowship (E.M.G.).

Earthquake Supercycles Inferred from Sea-Level Changes Recorded in the Corals of West Sumatra

Kerry Sieh,[1]* Danny H. Natawidjaja,[2] Aron J. Meltzner,[1] Chuan-Chou Shen,[3] Hai Cheng,[4] Kuei-Shu Li,[3] Bambang W. Suwargadi,[2] John Galetzka,[1] Belle Philibosian,[1] R. Lawrence Edwards[4]

Records of relative sea-level change extracted from corals of the Mentawai islands, Sumatra, imply that this 700-kilometer-long section of the Sunda megathrust has generated broadly similar sequences of great earthquakes about every two centuries for at least the past 700 years. The moment magnitude 8.4 earthquake of September 2007 represents the first in a series of large partial failures of the Mentawai section that will probably be completed within the next several decades.

Large sections of the great arcuate fault beneath the eastern flank of the Indian Ocean have failed progressively over the past 8 years in an extraordinary sequence of big earthquakes (Fig. 1) [1–4]. The largest of these failures of the Sunda megathrust, in 2004, caused the most devastating tsunami the world has seen in many generations. One question of great humanitarian and scientific importance is which remaining unruptured sections of the megathrust will fail next.

Until late 2007, the largest remaining unbroken Sumatran section had been the 700-km-long Mentawai patch, dormant since two great earthquakes in 1797 and 1833 [5]. Modeling of coral and instrumental geodetic data had shown most of the patch to have been highly coupled throughout at least the past half-century [6, 7]. That is, overlying and underlying blocks have been locked together, and strains continue to accumulate. These observations had led to concerns that the remainder of the Mentawai patch might rupture soon [8–11]. In September 2007, rapid-fire failure of portions of the Mentawai patch produced a moment magnitude (M_w) 8.4 earthquake and several large aftershocks [12], which served to further elevate anxiety.

[1]Tectonics Observatory, California Institute of Technology, Pasadena, CA 91125, USA. [2]Research Center for Geotechnology, Indonesian Institute of Sciences, Bandung, Indonesia. [3]Department of Geosciences, National Taiwan University, Taipei, Taiwan, ROC. [4]Department of Geology and Geophysics, University of Minnesota, Minneapolis, MN 55455, USA.

*To whom correspondence should be addressed at the Earth Observatory of Singapore, Nanyang Technological University, 639798 Singapore. E-mail: sieh@ntu.edu.sg

This paper shows that the history of the Mentawai section through the past few hundred years implies that the next large failure is likely to occur within the next few decades. We have extracted that history of strain accumulation and relief from corals on the fringing coral reefs directly above locked parts of the Sumatran megathrust.

Corals, growing just below the intertidal zone, record in their upper surfaces a history of local sea level (5, 7, 13–15). Annual lowest tidal levels limit the highest levels to which the coral colonies can grow (3), termed the highest level of survival (HLS) (13). Flat-topped pancake-like heads record sea-level stability. Heads with HLS surfaces that rise toward colony perimeters reflect rising sea levels during their decades of growth. This morphology inspired the name "microatolls" (16), diminutive analogs of Darwin's slowly drowning tropical islands that are or-

namented with an outer band of living coral reef (17). Changes in sea level recorded in microatoll HLS history reflect the lowering and raising of the islands in the course of elastic strain accumulation and relief. U-Th disequilibrium dating of coral can yield errors for uplift during earthquakes of just a few years (18–20).

Three paleoseismic sites, spanning 110 km of the Mentawai patch in the source region of the September 2007 earthquakes (Fig. 1 and fig. S1), show that major episodes of emergence (21) have occurred four times in the past 700 years.

At Bulasat, the first of the four emergences occurred in 1347 ± 18, the date of death of microatolls living at this and the Saomang site, a few kilometers to the south (Fig. 2A) [supporting online material (SOM), including figs. S1 to S7]. Undisturbed microatolls of this vintage rest at an elevation about 110 to 120 cm above our arbitrary datum, HLS in 2002.

The next emergence event occurred in 1607 ± 4, after decades of rapid submergence. Direct evidence for emergence in 1797 is not preserved in the corals at the Bulasat site. However, two microatolls at nearby Saomang (SOM,

including figs. S8 to S10) document relative sea-level rise of about 9 mm/year through part of the 17th and 18th centuries. These time series constrain the magnitude of uplifts in 1797 and 1833. Also, a microatoll at Saomang that died in 1833 yields a record for the early 19th century. This series' lack of colinearity with the records from the early 1700s reveals at least one emergence between about 1730 and 1810 (Fig. 2A). The most plausible date is 1797, the date of a historical large earthquake that is also clear in paleoseismic records at nearby sites (5). Extrapolation of these records implies emergence of about 1 m in 1797.

A living microatoll and continuous global positioning system (GPS) station at Bulasat yield comparable modern subsidence rates of ~13 and 15 mm/year. The GPS station recorded uplift of 73 cm during the September 2007 M_w 8.4 and 7.9 earthquakes (table S1B).

The Bulasat time series (Fig. 2A) resembles a saw blade. The tip of each sawtooth is the date of an emergence that presumably relates to a large earthquake, as in 2007. The back of each tooth is a ramp that slopes down to the date of the
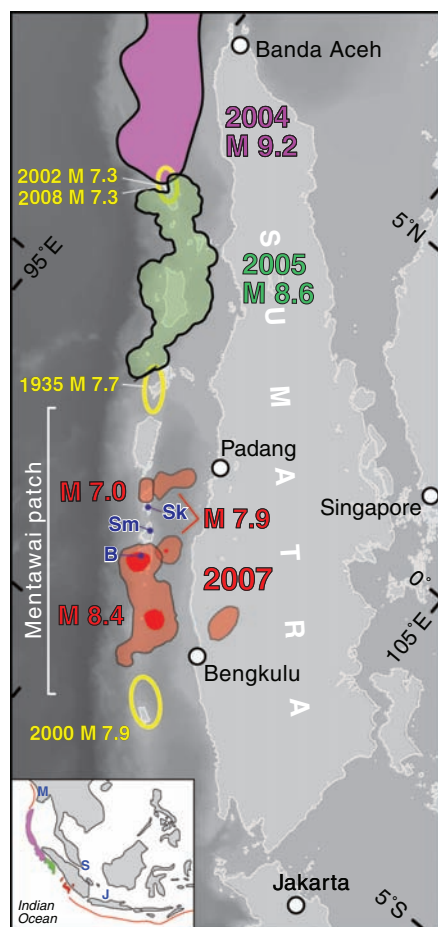
Fig. 1. Recent seismic ruptures of the Sunda megathrust, offshore of Sumatra, delineate highly coupled large (pink, green, and orange) and weakly coupled small (yellow) patches. The September 2007 sequence involved partial rupture of the Mentawai patch, which last broke in 1797 and 1833. B (Bulasat), Sm (Simanganya), and Sk (Sikici) indicate principal paleoseismic sites. Adapted from (1, 3, 5, 12, 15). (**Inset**) M, S, and J are Myanmar, Singapore, and Java. The red line is the Sunda megathrust.
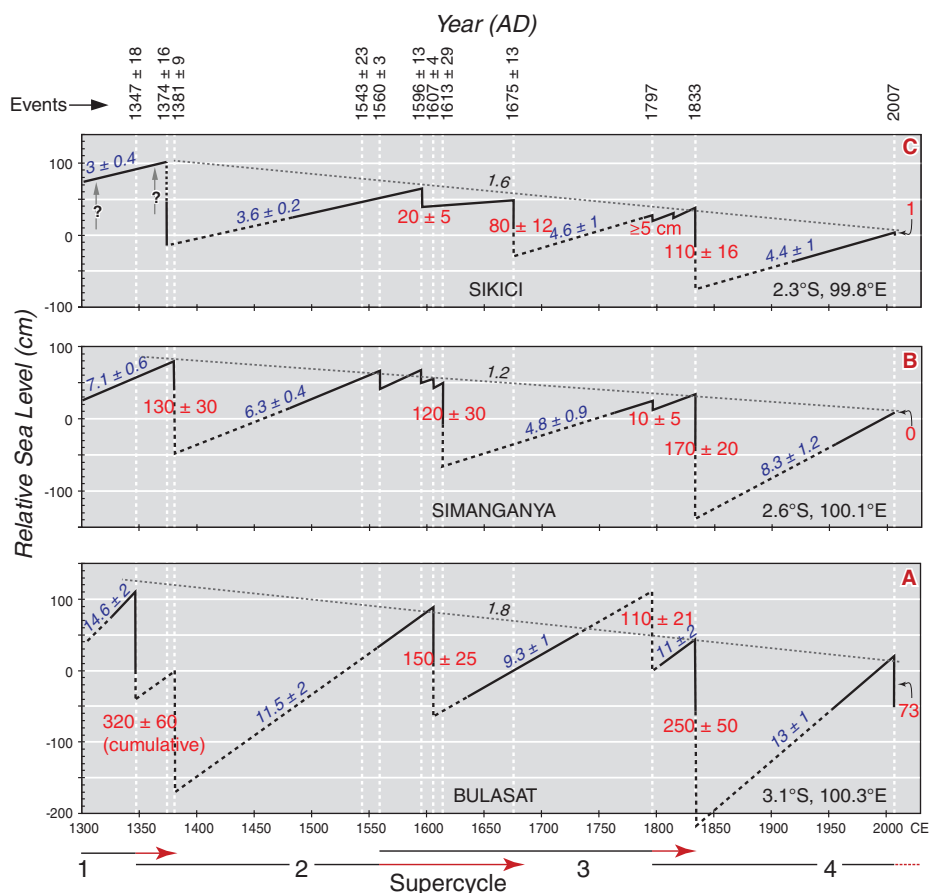

Fig. 2. Histories of interseismic submergence and coseismic emergence through seven centuries at sites (**A**) Bulasat, (**B**) Simanganya, and (**C**) Sikici. Data constrain solid parts of the curves well (fig. S4); dotted portions are inferred. Emergence values (in centimeters ± 2σ) are red. Interseismic submergence rates (in millimeters per year, ± 2σ) are blue. Millennial emergence rates are black. Vertical dashed white lines mark dates of emergences. Red arrows at bottom highlight the timing of the failure sequence for each supercycle.

previous earthquake. For the most part, the microatolls document the sloping part of the tooth for only a few decades before the earthquakes. The lack of data immediately after large earthquakes is a consequence of coseismic elevation of the entire reef flat above low tide levels if emergence is greater than about 1 m (22). At an interseismic submergence rate of 10 mm/year, one century is needed to bring each vertical meter of the reef flat back below low tide levels and able once again to support coral growth. Thus, we cannot rule out the possibility that the 3.2-m emergence of Bulasat in the mid- to late 1300s could have occurred in more than one closely timed event.

To estimate the magnitude of the pre-instrumental emergences, we extrapolate the interseismic subsidence rates back to the dates of the events (dotted sloping lines in Fig. 2A). Coseismic emergences are probably larger than the values given by linear extrapolation, because transient postseismic vertical deformation is commonly opposite in sign to the coseismic signal (23). However, this correction would probably be small; subsidence at GPS stations that rose 1.7 to 3 m during the great Nias-Simeulue mega-

thrust earthquake of 2005 has been only about 1% of the uplift value. And during the 6 months after the 73 cm of uplift in September 2007, only 2 cm of subsidence occurred at Bulasat.

The Simanganya site is about 60 km northwest of Bulasat, on the northeastern coast of North Pagai island (Fig. 1) (SOM, including figs. S11 to S24). The records at Simanganya and Bulasat are strikingly similar but not identical (Fig. 2).

The oldest large field of microatolls at Simanganya died late in the 14th century (Fig. 2B). The weighted mean date of death of five colonies is 1381 ± 9. This emergence appears to have occurred about one to six decades later than emergence at Bulasat.

The record of events around 1600 is complicated. Discordant elevations of 16th-century microatolls hint at significantly variable settling due to seismic shaking at the site. Thus, we use the elevation of the highest microatoll to infer sea level at the time of the first emergence, 1560 ± 3. Two microatolls constrain the magnitude of emergence to ~20 cm. The longest-lived microatoll records a large emergence in 1613 ± 29, preceded by two small emergences of ~10 and

>10 cm about 5 and 25 years earlier. Thus, Simanganya experienced three small emergences in the decades before the big event of about 1613.

One of the Simanganya microatolls records emergences that we associate with the 1797 and 1833 earthquakes (5). Its internal stratigraphy implies that emergence was about 10 cm in 1797. A modern specimen yields a record of submergence for the latter half of the 20th century. Linear extrapolation of this record back in time yields ~1.7 m of emergence in 1833. During the seismic episode of September 2007, vertical deformation at Simanganya was nil (table S1A).

At Sikici, on the northeast coast of Sipora island, large emergences occurred in the late 14th century, late in the 16th century, late in the 17th century, and in 1833 and 2007 (Fig. 2C) (SOM, including figs. S25 to S41).

Evidence for emergence in ~1374 appears in three microatolls that represent a large population. Although we chose these three colonies because of their relatively high degree of preservation and their nearly flat, untilted upper surfaces, the tops of these microatolls vary by tens of centimeters in elevation. This implies that their substrate
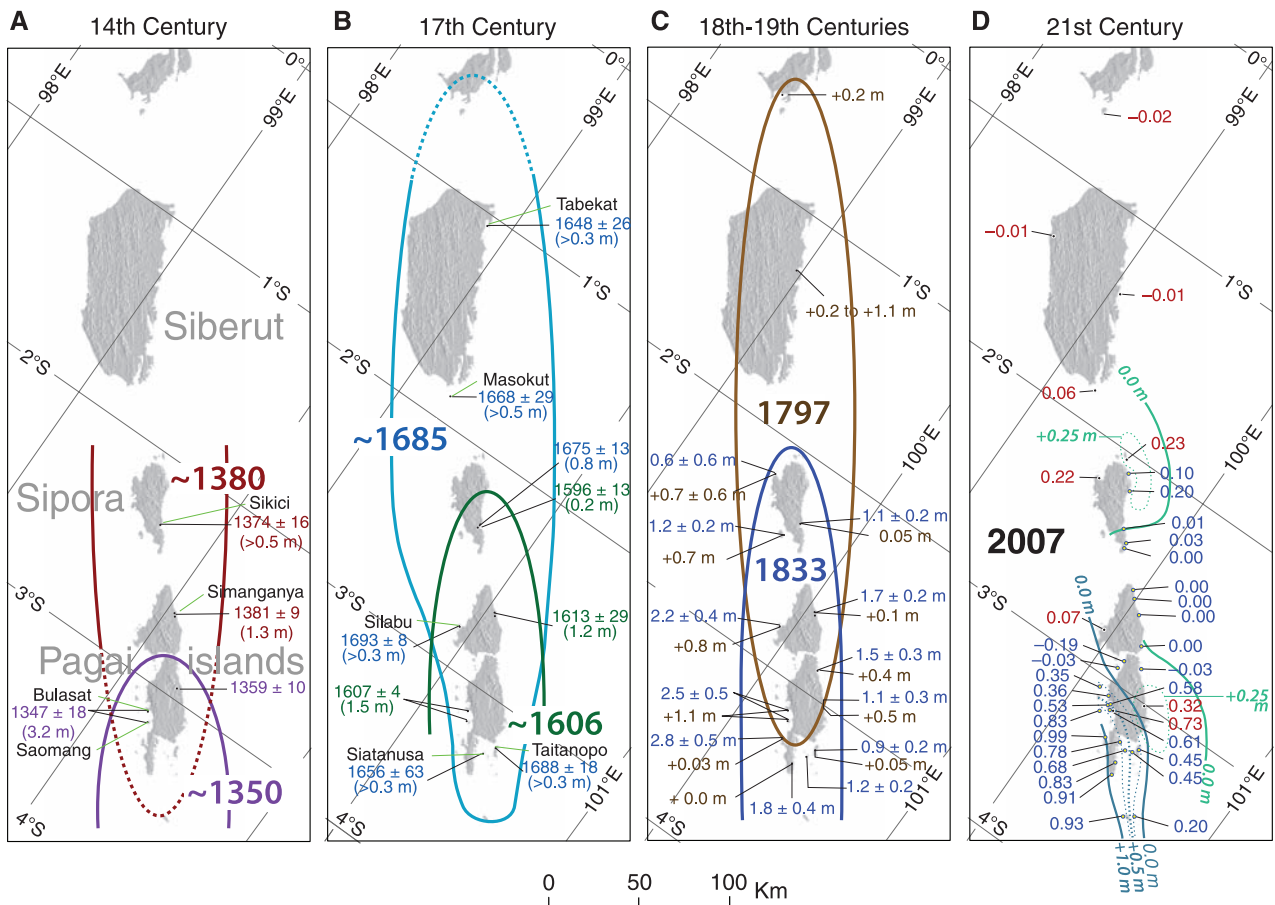

Fig. 3. Four emergence episodes of the past seven centuries. Each episode consists of more than one major event. (**A** and **B**) Emergence amounts are below the year of emergence (±2σ); colors indicate proposed event correlations. (**C**) Emergences attributed to the 1797 and 1833 earthquakes are brown and blue, respectively. (**D**) Uplift values for the 12 to 13 September 2007 sequence are red (GPS) and blue (coral). Contours of uplift in blue and green show the amounts attributable to the M_w 8.4 and M_w 7.9 events, respectively (SOM, including table S1). The 2007 events probably herald the beginning of the next failure sequence.

compacted to different degrees (fig. S4 and arrows in Fig. 2C). Compaction probably occurred during the seismic shaking associated with emergence, because younger microatolls do not display large elevation differences within their populations. The differing elevations of the 14th-century microatolls mean that we can say only that the original elevation of the population relative to modern sea level was at least as high as the highest colony.

Eight sampled Sikici microatolls record events of the 16th and 17th centuries. The best-preserved and dated records show slow sea-level rise from ~1480 to 1590, ~20 cm of emergence in 1596 ± 13, and a subsequent 80 years of sea-level stability, followed by another large emergence in 1675 ± 13. The living outer perimeters of four of the colonies were too thin to survive the 20-cm emergence of ~1596. The best-preserved of these four also show a small (6 cm) emergence 12 to 15 years before death. Such a small emergence could be tectonic, but an oceanographic cause is also plausible.

The 1797 and 1833 events appear in one sample (5). A 10-cm emergence 36 years before death appears to represent emergence in 1797. Extrapolation of a 4.4 mm/year rate of submergence from a modern microatoll (7) implies about 1.1 m of emergence in 1833. Within error, the magnitude of uplift (1 ± 6 cm) in September 2007 is nil (table S1A).

A few other localities also yielded useful, though shorter and less complete, records. Those that help constrain the 1797 and 1833 events are described in (5). Six others assist in piecing together the record before 1797 (SOM, including fig. S1).

The broadly similar sea-level histories of Bulasat, Simanganya, and Sikici imply similar histories of strain accumulation and relief on the underlying megathrust. Throughout the past seven centuries, all three sites have experienced interseismic submergence punctuated by correlated episodes of rapid emergence that are complex in both space and time.

The first emergence episode comprised two events, which occurred first at Bulasat and a decade or so later at the other two sites (Figs. 2 and 3A). The next episode began in ~1560 with a small emergence at Simanganya (Fig. 2B). In about 1600, all three sites rose suddenly (Figs. 2 and 3B). The largest emergence at Sikici was much later, ~1680. Emergence also occurred at about this time at Silabu, Siantanusa, and Taitanopo but could not have been more than about 10 cm at Saomang. Simanganya may also

have risen in ~1680, but the reef there might have still been too far out of the water to allow corals to be growing on the reef flat. Two microatolls (figs S42 and S43) suggest that this event extended as far north as Masokut and Tabekat.

Zones of emergence associated with both the great 1797 and 1833 earthquakes span all three major sites (Figs. 2 and 3C), but emergence in 1797 is much less than in 1833. Uplift in 2007 was 73 cm at Bulasat but nil at the other two sites.

Because each of the three past episodes of emergence consists of two or more discrete events, we refer to the broad periods of strain accumulation and relief as supercycles rather than merely cycles (Fig. 2). The corals record only the last few decades of supercycle 1 and only the strain-accumulation phase and initial part of the strain-relief phase of supercycle 4, but they capture all of supercycles 2 and 3.

At each site, emergence over each supercycle varies by no more than 40% (about 1 to 1.2 m at Sikici, 1.2 to 1.8 m at Simanganya, and 1.5 to 3.6 m at Bulasat). Sites with high emergence values are also sites with high rates of interseismic submergence. The largest events at each site are the last events in their failure sequence.

Emergences in 1797, 1833, and 2007 (Figs. 3C and 3D) are well-enough known to model the locations and magnitudes of slip on the megathrust. Tilt of the islands away from the trench implies megathrust ruptures under the islands that extend updip to the west (5, 12). The similarity of emergence values in 1797, 1833, and 2007 to those in earlier centuries suggests that megathrust slip in the earlier episodes was also centered beneath and west of the islands.

At each site, rates of interseismic submergence show little variation from supercycle to supercycle. This implies that the pattern of coupling (locking) on the megathrust defined by 20th-century coral and GPS data (6, 7) has persisted through the interseismic periods of the past several supercycles. The only major exception is Sikici's flat interseismic curve between ~1600 and 1680. This aberration may imply that the megathrust beneath Sikici was largely decoupled during those eight decades.

At least two of the three ancient failure sequences began with events that were smaller than their culminating events. Moreover, the megathrust rupture of September 2007 is far smaller than the amount of potential slip that has accumulated since the 1797-1833 couplet (Fig. 4 and fig. S44).
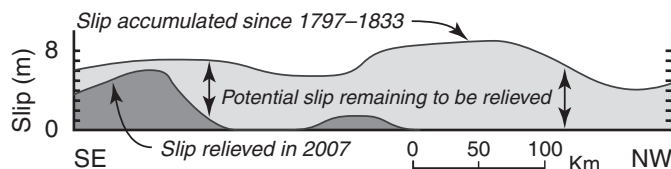
Failure initiation by smaller ruptures and the emergence of individual sites during both these and culminating large events imply either structural or rheological heterogeneity of the megathrust. As stresses approach failure levels, patches that are slightly more prone to failure yield first. The size of these patches may limit slip to less than the full 10 m or so of accumulated potential slip. Years or decades later, when the stronger patches fail, the remaining potential slip on the weaker patches is relieved in concert with slip on the stronger patches (Fig. 4 and fig. S44A). Thus, the culminating large earthquake has a larger magnitude than the initiating large earthquake. Because smaller earthquakes have also preceded some (24, 25), though not all, large modern ruptures elsewhere, this mechanism may commonly apply.

The 700-year record of Sumatran megathrust supercycles implies that the M_w 8.4 earthquake of 2007 was the beginning of an episode of failure of the Mentawai patch. If previous cycles are indicative of the one now in progress, the earthquakes of 2007 will turn out to be smaller than the culminating earthquake of supercycle 4. In fact, the amount of potential slip that was not relieved in September 2007 is enough to generate a M_w 8.8 earthquake.

This event would generate widely distributed strong seismic shaking in western Sumatra and would undoubtedly produce great damage in Padang and neighboring cities and villages. Moreover, models based on the rupture of rectangular sources under the Mentawais yield tsunami with several meters of overland flow depth along the coast at Padang and Bengkulu and 1 km or so of inundation distance (26). These results imply that losses of life and property could equal or exceed those in Aceh province in 2004.

Over the past 700 years, three episodes of emergence lasted variously from a few decades to a little over a century. This past variability precludes a precise empirical forecast of the next great earthquake and tsunami. Nonetheless, to those living in harm's way on the coasts of western Sumatra, it should be useful to know that the next great earthquake and tsunami are likely to occur within the next few decades, well within the lifetimes of children and young adults living there now.

References and Notes
1. M. Chlieh et al., Bull. Seismol. Soc. Am. **97**, S152 (2007).
2. H. R. DeShon, E. R. Engdahl, C. H. Thurber, M. Brudzinski, Geophys. Res. Lett. **32**, L24307 (2005).
3. R. W. Briggs et al., Science **311**, 1897 (2006).
4. R. E. Abercrombie, M. Antolik, G. Ekström, J. Geophys. Res. **108**, 2018 (2003).
5. D. H. Natawidjaja et al., J. Geophys. Res. **111**, B06403 (2006).
6. M. Chlieh, J.-P. Avouac, K. Sieh, D. H. Natawidjaja, J. Galetzka, J. Geophys. Res. **113**, B05305 (2008).
7. D. H. Natawidjaja et al., J. Geophys. Res. **112**, B02404 (2007).
8. K. Sieh, paper presented at the International Workshop on Tectonics of Plate Convergence Zones: Toward the Seamless Understanding from Earthquake Cycles to Geomorphic Evolution, University of Tokyo, Tokyo, Japan, 28 to 29 September 2006.

Fig. 4. Comparison of slip during the 2007 events and remaining potential slip on the Mentawai patch. The long axis is parallel to and through the Mentawai island chain. See SOM, fig. S44, and (12) for more details.

9. K. Sieh, *Philos. Trans. R. Soc. London Ser. A* **364**, 1947 (2006).
10. K. Sieh, paper presented at the First International Conference of Aceh and Indian Ocean Studies, Banda Aceh, Indonesia, 24 to 26 February 2007.
11. K. Sieh, *J. Earthquake Tsunami* **1**, 1 (2007).
12. O. Konca *et al.*, *Nature* **456**, 631 (2008).
13. J. Zachariasen, K. Sieh, F. W. Taylor, R. L. Edwards, W. S. Hantoro, *J. Geophys. Res.* **104**, 895 (1999).
14. J. Zachariasen, K. Sieh, F. W. Taylor, W. S. Hantoro, *Bull. Seismol. Soc. Am.* **90**, 897 (2000).
15. D. H. Natawidjaja *et al.*, *J. Geophys. Res.* **109**, B04306 (2004).
16. D. R. Stoddart, T. P. Scoffin, *Atoll Res. Bull.* **224**, 1 (1979).
17. C. Darwin, *The Structure and Distribution of Coral Reefs* (Smith, Elder and Co., London, 1842).
18. R. L. Edwards, F. W. Taylor, G. J. Wasserburg, *Earth Planet. Sci. Lett.* **90**, 371 (1988).
19. C.-C. Shen *et al.*, *Geochim. Cosmochim. Acta* **72**, 4201 (2008).
20. C.-C. Shen *et al.*, *Chem. Geol.* **185**, 165 (2002).
21. We use the terms "submergence" and "emergence" throughout to refer to changes with respect to a sea-level datum. We use "subsidence" and "uplift" in reference to other geodetic data and when inferring vertical tectonic motions.
22. K. Sieh, *Nature* **434**, 573 (2005).
23. Y.-J. Hsu *et al.*, *Science* **312**, 1921 (2006).
24. K. Sieh, M. Stuiver, D. Brillinger, *J. Geophys. Res.* **94**, 603 (1989).
25. G. Carver *et al.*, *Bull. Seismol. Soc. Am.* **94**, S58 (2004).
26. J. C. Borrero, K. Sieh, M. Chlieh, C. E. Synolakis, *Proc. Natl. Acad. Sci. U.S.A.* **103**, 19673 (2006).
27. This work has been supported by NSF grants EAR-9628301, 9804732, 9903301, 0208508, 0530899, 0538333, and 0809223 (to K.S.) and EAR-0207686

Shock Metamorphism of Bosumtwi Impact Crater Rocks, Shock Attenuation, and Uplift Formation

Ludovic Ferrière,[1] Christian Koeberl,[1]* Boris A. Ivanov,[2] Wolf Uwe Reimold[3]

Shock wave attenuation rate and formation of central uplifts are not precisely constrained for moderately sized complex impact structures. The distribution of shock metamorphism in drilled basement rocks from the 10.5-kilometer-diameter Bosumtwi crater, and results of numerical modeling of inelastic rock deformation and modification processes during uplift, constrained with petrographic data, allowed reconstruction of the pre-impact position of the drilled rocks and revealed a shock attenuation by ~5 gigapascals in the uppermost 200 meters of the central uplift. The proportion of shocked quartz grains and the average number of planar deformation feature sets per grain provide a sensitive indication of minor changes in shock pressure. The results further imply that for moderately sized craters the rise of the central uplift is dominated by brittle failure.
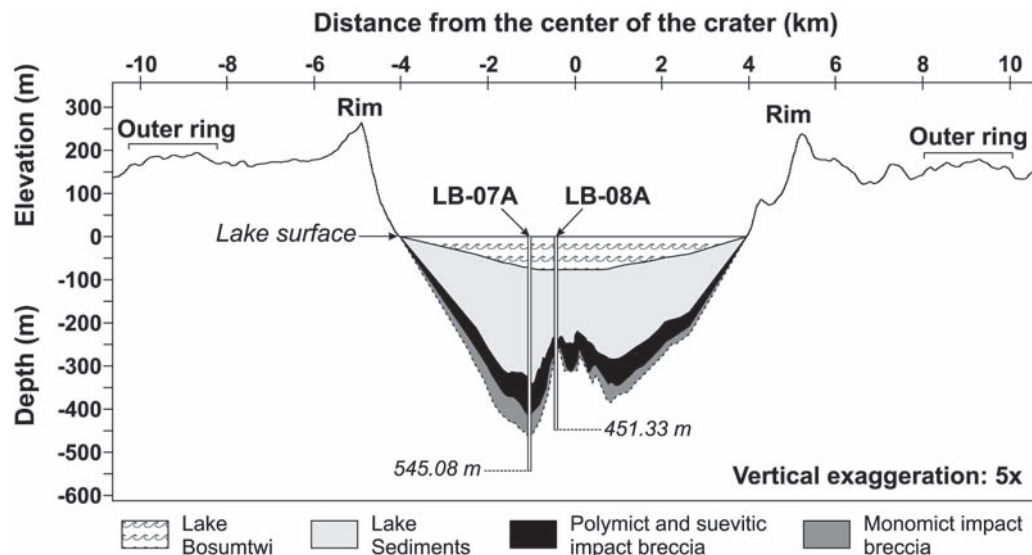
D uring the contact and compression phase of hypervelocity impact, a spherical shock wave is generated, propagates through the target rocks (*1*), and is attenuated rapidly with increasing distance. Consequently, a variety of shock effects are produced in rock-forming minerals, including formation of planar deformation features (PDFs) and high-pressure phases. The relative spatial distribution of these shock transformations and deformations formed at different pressures and temperatures [e.g., (*2*, *3*)] in autochthonous rocks, at the scale of the impact structure, can be used to estimate maximum shock pressures and, consequently, the rate of shock attenuation.

However, many parameters—such as rock type as well as lithological contrasts, texture, fabric, grain size, preshock orientation of grains, porosity, and volatile content—influence the shock levels attained locally. Furthermore, and typical in the case of complex impact structures (i.e., craters with diameters ≥2 to 4 km on Earth) (*4*), the original position and distribution of the shocked rocks is modified when, because of gravitational instability of the transient cavity rim, rebound of the crater floor leads to formation of a central uplift. Redistribution of rock is also associated with the collapse of the initially oversteepened central uplift (*5*).

There have been several efforts to estimate shock wave decay, mainly from nuclear and explosion crater studies or by numerical modeling [e.g., (*6*–*8*)]. Few studies have tried to quantify shock pressure distribution in simple (*9*) and complex impact structures (*9*–*16*) [see supporting

[1]Department of Lithospheric Research, University of Vienna, Althanstrasse 14, A-1090 Vienna, Austria. [2]Institute for Dynamics of Geospheres, Russian Academy of Sciences, Leninsky Prospect 38-1, 119334 Moscow, Russia. [3]Museum of Natural History (Mineralogy), Humboldt University, Invalidenstrasse 43, D-10115 Berlin, Germany.

*To whom correspondence should be addressed. E-mail: christian.koeberl@univie.ac.at

Fig. 1. Cross section of the Bosumtwi impact structure, based on Shuttle Radar Topography Mission (SRTM) data for the regional topography of the exposed portion of the crater (profile from west to east) and on a northwest-southeast seismic reflection profile (*21*) across the central crater. Location of boreholes LB-07A and LB-08A are given. The volume of lake sediments is based on seismic reflection data. The distribution of polymict and suevitic impact breccia and monomict impact breccia is based on observations from cores LB-07A and LB-08A (*19*, *20*), as well as interpretations of seismic reflection data. Depths and elevations are relative to lake level. SRTM data were available online (www2.jpl.nasa.gov/srtm/; accessed 3 March 2008).